The Role of Excipients and Package Components in the Photostability of Liquid Formulations

ROBERT A. REED, PAUL HARMON, DENISE MANAS, WALTER WASYLASCHUK, CHRIS GALLI, RYAN BIDDELL, PAUL A. BERGQUIST, WILLIAM HUNKE, ALLEN C. TEMPLETON and DOMINIC IP

Pharmaceutical Research & Development, Merck Research Laboratories, West Point, PA 19486

ABSTRACT: A phenyl ether-based drug substance exhibits photochemical degradation in citrate buffers with both ultraviolet (300–450 nm range) and visible light (380–700 nm range) exposure, even though the drug molecule itself is non-light absorbing at wavelengths >300 nm. The major contributors to the observed photosensitivity are the citrate buffer, parts per billion (ppb) levels of iron, oxygen, and light exposure level. Although a primary phenol photodegradate is generated, there are at least eight other species formed as well. The molecular weights and abundance of these species suggest that the product distribution is generated by the reaction of hydroxyl radicals with the drug substance. The generation of the primary photodegradate is linearly proportional to the light exposure amount for a fixed concentration of iron present in the formulation. Conversely, the amount of photodegradation is also nearly linear with iron concentration (through 200 ppb levels) for a fixed amount of light exposure. The proposed mechanism for the photochemical generation of hydroxyl radicals has precedence in the literature for similar combinations of iron, oxygen, carboxylate buffers, and light. Since the buffer salt and oxygen molecular equivalents in the product are significantly higher than the ppb levels of iron employed and more difficult to remove, the control of the extent of photodegradation largely rests on the control of trace levels of iron in the formulated product and control of light exposure. Exposure of drug solutions to a series of transition metals clearly indicates that iron is the key transition metal involved in the observed photochemistry. At manufacture, the primary source of iron is the raw materials (water, drug or excipients) used in the formulation. The level of iron for product stored in glass increases with sample age and can be attributed to iron leaching from borosilicate glass vials. Consideration of adequate light control during the manufacturing and packaging processes will be discussed and can only be defined as a function of the amount of iron present at the time of manufacture in the formulation. The generality of this chemistry to other drug candidates and in the presence of other common buffers will also be discussed.

KEYWORDS: Photostability, parenterals, polycarboxylates, Fenton chemistry, photocatalytic, iron-mediated photo-oxidation

Introduction

Iron plays a central role in biological systems (1). However, the solubility of Ferric ions is quite low in aqueous solution at neutral pH. In plants, animals and surface waters, low molecular weight polycarboxylates (such as citrate) serve to bind Ferric ions to form soluble complexes (2). While the ability of these complexes to undergo photolysis to generate Fe II was realized some time ago, most work has focused on aspects of the quantum yields for the Fe II generation, or on the fate of the carboxylate ligand (3). More recently, the potential effects of Fe II reaction with dissolved oxygen in solution has been considered (4, 5). In the latter cases, it was realized that generation of Fe II in oxygen saturated solutions may ultimately give rise to formation of hydrogen peroxide, which could then react with remaining Fe II to liberate hydroxyl radicals (6, 7):

$$Fe^{2+} + H_2O_2 \rightarrow Fe^{3+} + OH^- + \cdot OH \qquad (1)$$

The hydroxyl radicals can serve as a powerful oxidant capable of reacting with many organic compounds.

Corresponding Author: Robert A. Reed, Merck Research Laboratories, WP 78-110, P. O. Box 4, Sumneytown Pike, West Point, PA 19486; phone (215) 652-1691; email Robert_A_Reed@Merck.com

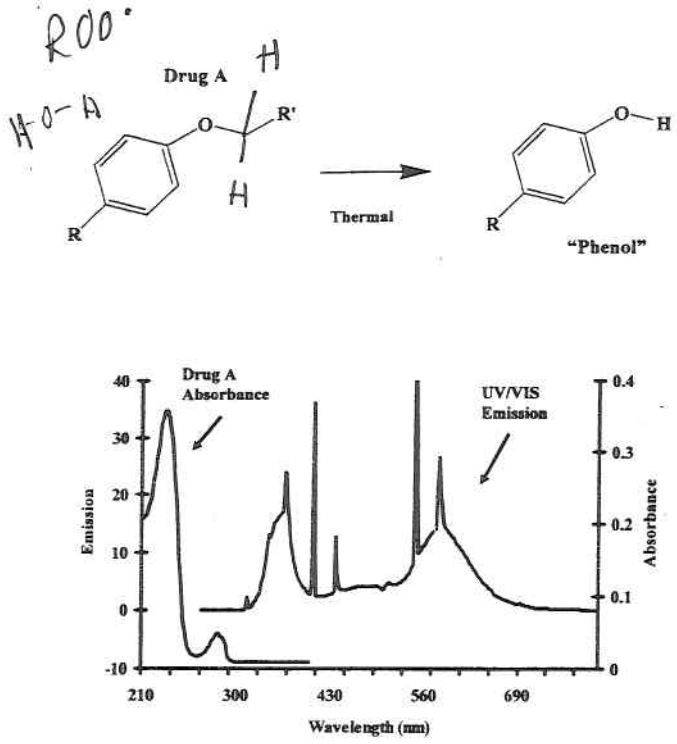

Figure 1

Top: Structures of Drug A and the known thermal degradation product, referred to as phenol in this report; Bottom: UV/VIS absorption spectrum of 0.064 mM Drug A in water compared to the spectral outputs of the ICH UV and visible lamps.

Recently, the International Conference on Harmonization (ICH) has provided guidance on the Photostability Testing of New Drug Substances and Products (Q1B) and highlighted the need to evaluate the photosensitivity of new pharmaceutical dosage forms (8). Strategies for improving the photostability of drug products have been suggested. Photochemical studies on the inherent photostability of drug substances and formulated products has also been reviewed in the literature (9–12).

The relevance of the body of literature on photochemical generation of Fe II from Ferric iron-carboxylate complexes to the recent ICH guidance on the photostability assessment of pharmaceutical products became apparent in our laboratories. Two pH 6 citrate buffer formulations of Drug A (a phenyl ether, shown in Figure 1, top), were found to be sensitive to light exposure when examined according to ICH-defined light conditions. The photosensitivity was unexpected, as there is negligible overlap of the Drug A absorption spectrum and either the ICH visible or UV lamp outputs (Figure 1, bottom). Furthermore, the molecular components of the matrix (Table I) are also non-light absorbing in the 300–700 nm exposure regions.

The objective of this paper is to explore the nature of the photosensitivity of this citrate-based formulation and to examine the generality of the experimental observations to a larger class of buffer systems and, in general, to liquid dosage forms. Additionally, the role of the formulation excipients and package components will be discussed, as well as the implications of the needed control of light in manufacturing and packaging operations.

Materials and Methods

Materials

The phenyl ether-based drug substance (Drug A), the phenyl piperidone-based drug substance (Drug B), the alkyl piperidone drug substance (Drug C) and the phenyl thiazole drug substance (Drug D) were provided by Merck & Co., Inc. (Whitehouse Station, NJ). Sodium chloride and sodium citrate were purchased from Mallinckrodt Chemical Inc. (St. Louis, MO). Citric acid was purchased from Fisher Scientific (Pittsburgh, PA). Disodium maleate, disodium succinate, sodium formate, sodium oxalate and sodium tartrate were all purchased from Aldrich (Milwaukee, WI).

TABLE I
Summary of the Two Product Formulation Compositions for Drug A Examined in This Study

Component	Formulation I		Formulation II	
	mM	Relative Molar Amount[a]	mM	Relative Molar Amount[a]
Drug A	0.57	1.0	0.11	1.0
Citric Acid	0.8	1.5	0.17	1.5
Sodium Citrate	9.2	16.2	1.83	16.2
Sodium Chloride	136	241	153	1357

[a] Molar ratio of specified component relative to Drug A free base.

Zinc sulfate, copper sulfate, nickel sulfate, manganese chloride, cobalt chloride, iron (II) chloride and iron (III) chloride were all purchased form Fisher Scientific (Pittsburgh, PA). All materials were used as received.

Buffer Solutions

All buffer solutions were prepared in deionized water at 10 mM concentrations and adjusted to the specified pH with the addition of 1N HCl (Fisher Scientific, Pittsburgh, PA). Zero to 1000 parts per billion (ppb) levels of iron chloride and 100 ppb levels of other transition metals were added as desired to the solutions as salts.

Stability Analysis

The purity profile of the product was assessed on a ThermoSeparations HPLC (ThermoQuest, San Jose, CA) equipped with a P4000 quaternary pump, an AS4000 auto sampler, and a UV3000 detector. All Drug A analyses were performed on a Waters (Milford, MA) Symmetry C18 column using an acetonitrile/pH 3 phosphate buffer mobile phase with UV detection at 227 nm.

Transition Metal Determinations

Initial semi-quantitative analysis of 10 mM citrate buffer solutions was performed on an HP Inductively Coupled Plasma-Mass Spectroscopy Instrument (Model HP 4500). Final quantitative measures were then taken on a Perkin-Elmer ICP/OES instrument (Optima 3300DV) for the determination of iron in each buffer solution. The method was validated to measure to 5 ppb levels of iron, and quantitation was achieved using the method of standard addition. Typically, iron levels were measured both pre- and post-addition of a known quantity of iron (III) chloride.

Photostability Determinations

Photostability studies were performed using a calibrated ICH ES2000 (Environmental Specialties, Inc., Raleigh, NC) photo-chamber equipped with both a UVA and cool white fluorescent bulb (ICH, Option 2) to allow independent exposure to both UV and visible spectral regions. Typical exposure conditions were 108 Kilo Lux and 20W/m^2 for cool white and UVA light exposure, respectively. The orientation of the sample in the chamber was found to be insignificant to the qualitative and quantitative aspects of the photodegradation. Dark controls were performed with each study to confirm the absence of thermal contributions by either wrapping control samples in aluminum foil or by placing control samples in a light-protective carton. The chamber was maintained at 25°C and ambient humidity (~40% RH) for all measurements. The variability in light exposure was less than 10% (International Light IL 1400A radiometer) for all experiments. Yellow light exposure conditions were imitated by covering the lights in the chamber with a yellow film (3-mm thick Amber 3, Cat. No. 362931902U, Team Plastics, Cleveland, OH), keeping the light exposure time fixed.

Photochemical Product Characterization

Photodegraded Drug A solutions were concentrated and the buffer removed by solid phase extraction methods. Drug A solutions were passed through a Sep-Pak C18 cartridge (Waters Corp., Milford, MA) which retained all degradation products and the parent compound. The cartridge was then washed with water to remove the buffer salts, and then the Drug A related species were eluted with acetonitrile. The acetonitrile was then removed and the sample resuspended in the following LC-MS compatible mobile phase: 88/12, 1 mM acetate buffer (pH 2.6) /acetonitrile. This mobile phase was used to isocratically elute the Drug A-related species into a Finnigan LCQ Mass spectrometer (San Jose, CA) Electrospray Ionization, in positive ion mode.

Results

Solution Photostability

Initial ICH photostability studies on a Drug A (Formulation I, Table I) solution showed the surprising results typified by the chromatograms in Figure 2. The upper chromatogram in Figure 2 is from a Formulation I solution contained in a clear glass vial and exposed to the ICH recommended UV (200 Watt-h/m^2) and visible (1.2 million lux-h) light doses. The phenol degradation product is clearly evident and is present at about 0.7%. Other earlier eluting species are evident which cannot be attributed to diluent peaks or process impurities. The lower chromatogram in Figure 2 shows an identical sample first placed in a protective carton then exposed to the same ICH light conditions. The phenol peak is absent, as are the earlier eluting species. Clearly, light exposure affects the stability of this drug solution and gives rise to elevated levels of the phenol "thermal" degradation product. Similar behavior was observed for Drug A Formulation II (Table I).

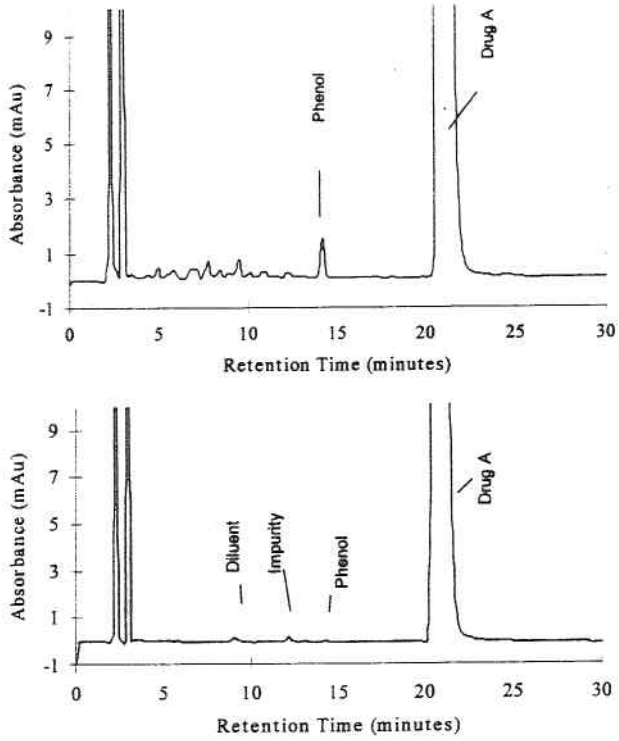

Figure 2

Results of the photostability study conducted on a 0.57 mM Drug A, 10 mM citrate (pH 6), 136 mM sodium chloride solution. The lower chromatogram is that of product exposed to full ICH conditions protected in an individual carton. The upper chromatogram is that of product exposed in a clear USP Type I glass vial. Note that the unprotected sample shows several extra peaks, the most prominent being the phenol.

Effects of Incremental Light Exposure

The effect of incremental light exposure levels was examined for Formulation I solutions for both visible and UV light by titrating the amount of light through full ICH exposure levels. Visible light was increased through 1.2 million lux-h in 0.3 million lux-h increments. UV light was increased through 200 W-h/m^2 in 50 W-h/m^2 increments. The plot in Figure 3 shows the loss of Drug A levels (-•-) as well as the increase in % phenol (-■-). Additionally, total degradation products were attempted to be integrated, including the earlier eluting peaks as well as phenol (4 to 15 minute retention time range, data not shown). Drug A decreases linearly with visible and UV light exposure from about 101% to 96% levels through full ICH UV and visible light exposure. Total degradation products increase to near 2%. There may be even earlier eluting unresolved species. The plot in Figure 3 shows the phenol levels specifically, which increase linearly with UV and visible light exposure to 0.7% levels at full ICH exposure. The quantitative results of this study, as well as the light exposure conditions given, are summarized in Table II.

Variation in Photosensitivity from Preparation to Preparation

Throughout the course of these studies, multiple batches of the same formulation were exposed to either full ICH exposure conditions or only the visible component of ICH light, as indicated in Table III. The measured phenol levels were seen to vary somewhat for a given batch and perhaps reflect the variation in the experiment. For example, for batch 2 with full ICH exposure, two values were generated in one light chamber, and both yield 0.7% phenol levels. Vials exposed in an equivalent, but different, ICH chamber resulted in 0.4% levels of phenol. However, substantial variation is observed between different preparations of the formulation. One major trend appears to be that older formulation solutions are more photosensitive than recently prepared solutions (*vide supra*). This trend is shown clearly by the chromatograms in Figure 4. After ICH visible exposure, a 3-month-old solution has about 0.1% levels of phenol, a 13-month-old solution forms 0.4% phenol, while a 23-month-old solution forms 1.2% phenol.

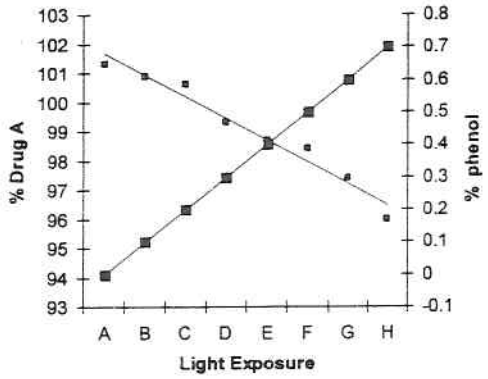

A= 0.3 million lux hours
B= 0.6 million lux hours
C= 0.9 million lux hours
D= 1.2 million lux hours
E= 1.2 million lux hours followed by 50 W hrs/m^2
F= 1.2 million lux hours followed by 100 W hrs/m^2
G= 1.2 million lux hours followed by 150 W hrs/m^2
H= 1.2 million lux hours followed by 200 W hrs/m^2

Figure 3

Photodegradation induced by ICH light exposure for a 0.57 mM Drug A, 10 mM citrate (pH 6), 136 mM sodium chloride solution. Note the decrease in Drug A levels versus the increase in phenol levels.

TABLE II
Summary of Photodegradation Results through ICH Recommended Light Exposure

Exposure Condition		% of Component Found		
Visible (lux-hours)	UV (Watt-hrs/m^2)	Drug A	Phenol	Total Degradation Products
0.3 million	0	101.3	<LOQ	<LOQ
0.6 million	0	101.0	0.10	0.10
0.9 million	0	100.6	0.21	0.33
1.2 million	0	99.3	0.31	0.81
1.2 million	50	98.8	0.40	1.13
1.2 million	100	98.3	0.48	1.35
1.2 million	150	97.4	0.60	1.58
1.2 million	200	96.0	0.71	1.86

The large magnitude of the variation in photosensitivity observed for different manufactured batches as well as for bench top preparations (Table III) argues that the photodegradation is not a function of a component that is intentionally controlled in the formulation. If, for example, the photo-instability were coming directly from Drug A light absorption, it would be difficult to account for a 10-fold variation in the percentage of phenol levels formed upon a given ICH exposure. Further evidence that Drug A is not the absorbing species is the very poor spectral overlap between its' absorption (extending to only 300 nm) and the output of the ICH visible lamp, as shown in Figure 1. Indeed, even the ICH UV lamp has very weak output, near 300 nm, yet both the UV *and* visible lamps promote the photodegradation.

Contribution of Excipients to Photosensitivity: The Role of Citrate

Additional experiments were performed to determine the role excipients play in the photodegradation process. Formulations were made in the laboratory that

TABLE III
Lot-to-Lot Variability in Photodegradation of 0.57 mM Drug A, 10 mM Citrate (pH 6), 136 mM Sodium Chloride Solutions with ICH Recommended Light Exposure

Lot Identification	Source of Solution Preparation	% of Phenol Observed					
		Full ICH Exposure[a]			Visible Exposure Only[b]		
		Run #1	Run #2	Run #3	Run #1	Run #2	Run #3
Batch one	Manufacturing	2.0%			1.2%		
Batch two	Manufacturing	0.4%[c]	0.7%	0.7%	0.3%	0.2%	0.4%
Batch three	Manufacturing	0.3%			0.1%		
Batch four	Laboratory[d]				<0.1%		
Batch five	Laboratory[e]	0.2%					
Batch six	Laboratory[e]	1.0%					
Batch seven	Laboratory[e]	0.3%					

[a] 200 Watts/meter squared of UV light and 1.2 million lux-hours of visible light exposure.
[b] 1.2 million lux-hours of visible light exposure.
[c] Exposure was done using a photo-chamber at another facility. The remainder of the exposures were performed at Merck Research Laboratories.
[d] Lot was prepared in a laboratory and 1.4 million lux-hours of visible light exposure was provided.
[e] Lot was prepared in a laboratory.

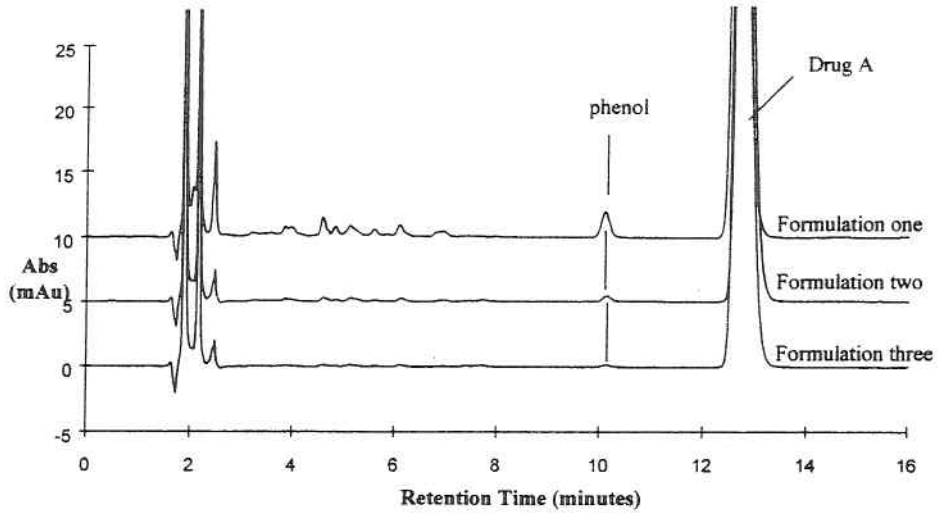

Figure 4

Chromatograms after 1.2 million lux of visible exposure, Lower, 3-month-old lot; middle, 13-month-old lot; upper, 23-month-old lot. Note increasing level of phenol.

consisted of 0.57 mM concentrations of Drug A in 1) 10 mM citrate (pH 6) and 136 mM sodium chloride, 2) 136 mM sodium chloride, 3) deionized water, and 4) 10 mM phosphate (pH = 6) buffer. The four solutions were then placed in clear, 50 mL USP Type I glass vials, stoppered and placed in the ICH photochamber and given full ICH light exposure. Photodegradation (0.2% levels of phenol) with full ICH light exposure was observed only for the sample containing citrate. The other three sample preparations did not show any evidence of photodegradation. In a second experiment, samples were prepared containing 0.57 mM Drug A in 10 mM citrate, both with and without 136 mM sodium chloride. Both solutions demonstrated equivalent levels of photodegradation upon exposure to full ICH light conditions. These studies showed that citrate plays a key role in the photosensitivity of Drug A. However, citrate absorption also shows no overlap with ICH visible lamp outputs, and the variation in magnitude of photosensitivity discussed above is not consistent with citrate alone as the photoreactive agent.

Analysis of Degradation Product Structures Implicates Formation of Hydroxyl Radicals

At this point, it was realized that the photodegradation process might be complex. The appearance of many earlier eluting species along with the phenol (Figure 2, upper chromatogram; Figure 4, middle and upper chromatograms) provided an opportunity to investigate the photodegradation mechanism. The structures of the early eluting species were therefore investigated by LC-MS and UV spectroscopy. The UV spectra of all the photodegradates were similar to the Drug A parent compound except one, which suggested an additional conjugation of the phenyl ring. Eight species (in addition to the phenol) could be assigned a molecular weight from the LC-MS analysis. Four species have molecular weight gains of 16 mass units over the Drug A parent compound. This mass gain is typical of a C–H bond being converted to C–OH bond. Three additional species showed mass gains of 14 mass units, which are interpreted to be conversion of a methylene group ($-CH_2-$) to a ketone (C=O) group. One of the 14 mass gain species showed the conjugated phenyl ring absorbance. Finally, a species showing a +32 mass unit gain over the Drug A parent was observed. This species could result from conversion of a C–H group to a peroxy group C–OOH or from two C–H bonds being converted to C–OH bonds.

The types of new bonds being formed argue that hydrogen atoms of C–H bonds of Drug A are being abstracted by an oxygen-centered radical. The large number of sites of hydrogen atom abstraction further argues that the oxygen-centered radicals are not likely hydroperoxy or peroxy radicals (HOO• or ROO•) since these radicals are quite selective in their reaction

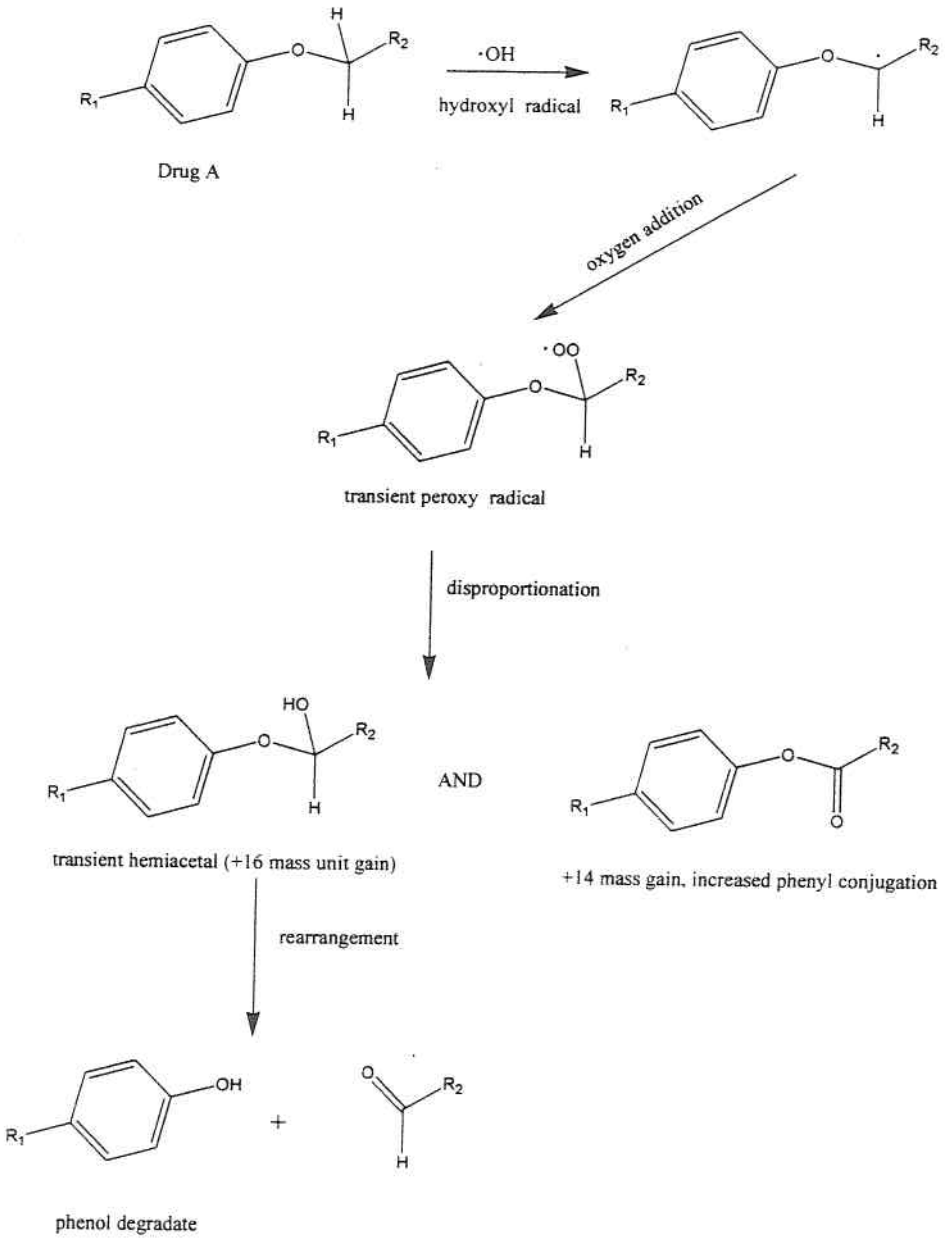

Figure 5

Reaction of hydroxyl radical with Drug A to produce phenol degradate and a +14 mass unit gain species with extended phenyl conjugation. Hydroxyl radical abstracts a hydrogen atom leaving a carbon centered radical, to which dissolved oxygen quickly adds to give a peroxy radical. Disproportionation gives an alcohol and a carbonyl species at the original site of hydrogen atom abstraction. In the specific case of the carbon atom shown here, the alcohol is unstable and rearranges to the phenol degradate.

with C–H bonds. Indeed, Drug A is stable when exposed to peroxy radicals. In contrast, the rich product distribution could be explained by the encounter with hydroxyl radicals (HO•), which are much less selective. Abstraction of Drug A C-H hydrogen atoms by hydroxyl radical, followed by oxygen addition, would generate transient peroxy radicals, which would then largely disproportionate since Drug A is stable toward peroxy radicals. Disproportionation of the peroxy radicals should then yield equivalent amounts of alcohol C-OH and carbonyl C=O products at each C–H bond site. The dominant 16 and 14 mass unit gains characteristic of the product distribution observed here are consistent with this general pathway and can also account for the formation of the phenol species, as shown in Figure 5.

Superoxide Radical Formation

$$Fe^{2+} + O_2 \Longrightarrow Fe^{2+}{-}O_2 \Longrightarrow Fe^{3+}{-}O_2^- \Longrightarrow Fe^{3+} + O_2^-$$

Superoxide Radical Protonation to Hydroperoxyl Radical

$$O_2^- + H^+ \Longrightarrow {}^{\cdot}OOH$$

Recombinations to Give Hydrogen Peroxide

$$O_2^- + H^+ + {}^{\cdot}OOH \Longrightarrow H_2O_2 + O_2$$

$$^{\cdot}OOH + {}^{\cdot}OOH \Longrightarrow H_2O_2 + O_2$$

Fenton Reaction Liberating Hydroxyl Radicals

$$Fe^{2+} + H_2O_2 \Longrightarrow Fe^{3+} + {}^{\cdot}OH + OH^-$$

Figure 6

Scheme for reduced iron reacting with oxygen to form superoxide and ultimately hydrogen peroxide. Reduced iron then reacts with hydrogen peroxide to liberate hydroxyl radicals.

Formation of Reduced Iron Species Implicated

Possible sources of hydroxyl radicals were considered. The formation of hydroxyl-type radicals as a result of Drug A absorption was considered unlikely as described above. One potential source of hydroxyl radicals is known which culminates with reaction (1); this process is depicted in Figure 6. The reduced form of some transition metals, the most notable and abundant being iron, can react with dissolved oxygen in solution to give superoxide radical, O_2^- (1, 4). Superoxide radicals can then protonate in water to generate hydroperoxyl radicals. A number of recombinations can then occur to give hydrogen peroxide, H_2O_2. Once hydrogen peroxide is formed, reaction with reduced iron to give hydroxyl radicals (Figure 6) is well known and serves as the basis of Fenton's reagent (4–6). That the pathways depicted in Figure 6 are leading to the complex Drug A degradation profile was easily demonstrated by simply adding a few hundred ppb of reduced iron (Fe II) to Drug A Formulation I solutions. Even in the dark, the "photodegradation" profile was faithfully reproduced.

Further, it was determined that spiking of Fe (III) into Drug A product only gave rise to the degradation profile upon exposure to light. One hundred ppb iron in the form of Fe^{3-} chloride was spiked into the 23-month-old product lot and subjected to ICH visible stressing. The bottom chromatogram in Figure 7 shows the unspiked product (from Figure 4, upper chromatogram), while the upper chromatogram shows the 100 ppb Fe^{3+} spike. The same early eluting peak pattern is reproduced, along with increased phenol levels. The photodegradation caused by spiking Fe^{3+} also shows the same citrate and light dependence described above, that is, in Drug A solutions in phosphate buffer, added Fe^{3+} does not promote degradation upon ICH visible exposure, and Fe^{3+} spiked into Drug A citrate solutions does not promote degradation if the product is kept in the dark. These results indicate the combination of citrate and light exposure must promote the reduction of Fe^{3+} to Fe^{2+} allowing the reactions in Figure 6 to proceed.

Citrate and Photons as Iron-reducing Agents

The reactions depicted in Figure 6 were implicated further when it was realized that the photoreduction of Fe^{+3} citrate complexes to Fe^{+2} is known in the literature and that hydroxyl radical formation has been reported (8) from such systems (3–6). Citrate will form a metal chelate with Fe^{3+}. Quantum yields for the photoreduction of these types of Fe^{3+} carboxylate complexes have been reported in the literature (3, 5) and are pH-dependent. For the case of Fe^{3+} citrate complexes specifically, quantum yields appear higher near pH 4 and decrease near pH 2 to 3; across the pH

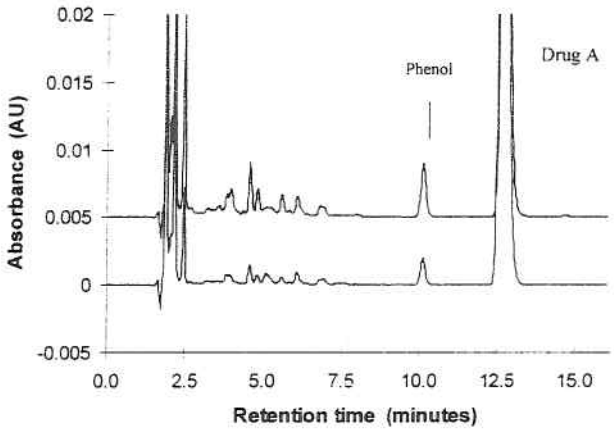

Figure 7

Chromatogram of 100 ppb Fe^{+3} spike (TOP), overlayed with 2-year-old unspiked (BOTTOM). Note similarity in peak elution patterns.

2 to 5 range values of about 0.1 to 0.3 can be expected in the 400–450 nm spectral range (3, 5). In contrast, it is interesting to note that the recombination reactions leading to hydrogen peroxide in Figure 6 will proceed more readily at lower pH. Thus, the overall pH dependence of the hydroxyl radical generation cannot be readily predicted. To this end, the pH dependence of phenol formation was examined in Drug A Formulation I solutions over the 2 to 6 pH range after exposure to 1.2 million lux hours of ICH visible light. Figure 8 shows the overall pH dependence of the photodegradation for a fixed iron concentration and light exposure.

This mechanism for Fe^{3+} reduction to Fe^{+2} explains the citrate dependence, as well as the seemingly odd wavelength dependence of the observed Drug A photo-instability. The spectral output of both ICH UV and ICH visible lamps have intensity in the 400–450 nm spectral region in which the Fe^{3+} citrate complex quantum yields have been reported. The relative spectral emissions from these lamps are shown in Figure 9. Also shown in Figure 9 is the absorption spectrum of the Fe^{3+} citrate complex obtained by preparing 0.1 mM Fe^{3+} in the presence of 10 mM citrate. Figure 9 thus provides a rationale for why the UV and visible ICH stressing conditions will both lead to the observed photodegradation, as Fe^{3+} can be photoreduced to Fe^{2+} in the presence of citrate by either lamp output.

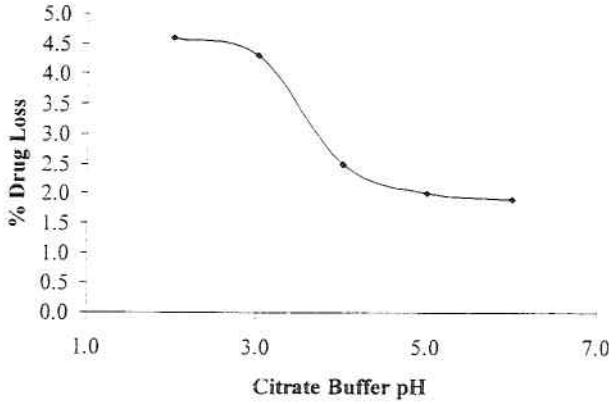

Figure 8

Percentage of drug loss observed for 0.57 mM Drug A in 10 mM citrate buffer (pH adjusted from 2.0–6.0) after exposure to ICH visible lamp (1.2 million lux hours) in the presence of 10 ppb iron.

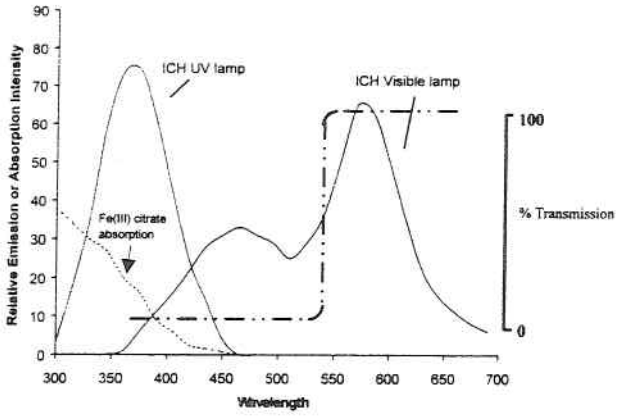

Figure 9

Spectral outputs for ICH visible and UV lamps with Hg emission lines removed, solid lines, and the Fe^{3+} citrate complex absorption spectrum. Note overlap of both ICH lamps with 400-450 nm Fe^{3+} citrate complex absorption (------). Also, note transmission properties of the yellow light filters (—·—·—) used in this study and common to many manufacturing areas.

The Role of Oxygen

Further experiments were carried out to determine if the degradation caused by adding Fe^{3+} to Formulation I followed by light exposure was dependent on oxygen, as predicted by the reaction schemes in Figure 6. Relatively large amounts of iron had to be added to clearly see the effect of oxygen removal by sparging the sample with helium for about 30 minutes. For example, 1000 ppb levels of Fe^{3+} were spiked into two Formulation I samples. One vial was sparged with helium to reduce the oxygen content, while the other vial was unsparged. After ICH visible stressing, the sparged vial showed about 8-fold less degradation than the unsparged case, in which about 50% of Drug A degraded. If no iron was added, similar sparging failed to substantially reduce the photodegradation. This is readily explained by the relative molar amounts of oxygen and Drug A molecules in solution, as shown in Table IV. When 1000 ppb iron is added, the molar amount of Drug A that is converted to other species is about 25% of the total oxygen in solution. Getting rid of ~90% of the dissolved oxygen in this case has an effect. In the unspiked lot, only a few percent of Drug A is degraded, corresponding to about 1% of the dissolved oxygen on a molar basis. Thus, sparging will be much less effective in prohibiting the photodegradation.

TABLE IV
Molar Ratios of 0.57 mM Drug A, 10 mM Citrate (pH 6), 136 mM Sodium Chloride Formulation Components Normalized to 50 ppb Iron

Component	Formulation I		Formulation II	
	mM	Relative Molar Amount[a]	mM	Relative Molar Amount[a]
Drug A	0.57	641	0.11	126
Citric Acid	0.8	925	0.17	185
Sodium Citrate	9.2	10200	1.83	2040
Sodium Chloride	136	152222	153	171086
Oxygen	1.3	1444	1.3	1444
Iron	50 ppb	1.0	50 ppb	1.0

[a] Molar ratio of specified component relative to 50 ppb iron.

Iron Found To Be the Most Abundant Transition Metal

Drug A formulation lots were then examined for evidence of iron as well as other transition metal ions. Inductively coupled plasma-mass spectroscopy (ICP-MS) was used initially in a semi-quantitative scanning mode. This mode of detection allows for determination of the elements sodium through mercury with detection limits of about 1 ppb with absolute errors typically about ±30%. The three manufactured batches shown in Table III and Figure 4 were examined. With the exception of iron, no first, second or third row transition metal ion was found in any lot at greater than 2 ppb. Most transition metals were undetectable. Iron, in contrast, was detected at between 10 and 30 ppb. Iron levels were quantitated more accurately by using the method of standard addition and by subtracting out m/z = 57 interferences due to argon oxides in the plasma. A standard addition curve was generated by spiking in 50 and 100 ppb Fe^{3+} into batch one, along with measurement of the unspiked lot. The iron isotope monitored was the m/z = 57 species. The interference at the same m/z ratio due to an argon oxide isotope was corrected by subtracting the m/z = 57 counts obtained for a 136-mM sodium chloride blank from all samples. Extrapolation of a linear fit back to the x-axis gives a concentration of about 40–45 ppb iron in the unspiked, 23-month-old batch 1, 10–15 ppb iron in the 13-month-old batch 2, and 0–5 ppb in the 3-month-old batch 3. The 5 ppb range in each measurement reflects estimates of possible error due to the background correction, as well as the possibility of up to 3 ppb iron levels in the sodium chloride blank. Table V shows the batch ID, lot age, and ppb iron level using the 5 ppb iron range determined from the ICP-MS measurements.

Increasing Iron Levels Correlate with Drug A Product Lot Photosensitivity

The increase in iron levels in the three lots examined by ICP-MS correlates quite well with the observed photosensitivity of each lot. This is demonstrated by the overlapping nature of the two plots in Figure 10. The square data points show the ppb iron determined by ICP-MS from Table V, while the circular data points show the percentage of phenol formed in each lot from visible ICH exposure (Table V). The agreement between the two is excellent. Additionally, the percentage of Drug A loss was examined for formu-

TABLE V
Lot ID, Age, Levels Phenol and ppb Iron by ICP-MS/OES

Lot ID	Age of Lot at Testing	Phenol Levels[a]	ppb Iron[b]
Batch one	23 months	1.2%	45
Batch two	13 months	0.4%	15
Batch three	3 months	0.1%	5

[a] Levels of % phenol after 1.2 million lux hours of visible light exposure.
[b] Iron levels were determined by ICP/OES.

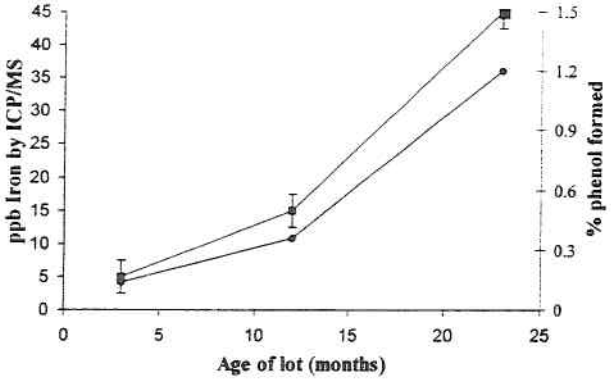

Figure 10

Dual plot of phenol resultant of 1.2 million lux-hours of visible light exposure and ppb iron levels determined for the same three lots by ICP-MS/OES (data from Table V).

lation I as a function of added iron (III) up through 1000 ppb levels (Figure 11) after full ICH visible light exposure. The observed photodegradation demonstrates a linear correlation up through about 200 ppb levels of added iron, then it becomes increasingly non-linear.

Further evidence of the correlation between iron levels and the extent of Drug A photodegradation is that phenol levels, for example, accurately predict iron content. From Figure 11, the percentage of phenol measured in batch one with zero, 100, and 200 ppb iron added upon ICH visible exposure, if treated as a "standard addition" curve followed by extrapolation back to the x-axis using a simple polynomial fitting, gives an estimate of about 50 ppb iron in the unspiked sample. The 50-ppb iron value based on phenol levels is in excellent agreement with the 40–45 ppb iron levels determined by the ICP-MS methods for the same lot. The agreement supports the unique role of iron as the transition metal responsible for the observed photosensitivity.

Rationale for Increasing Iron Levels

The rationale for increasing levels of iron with the age of Drug A, 10 mM citrate (pH 6), 136 mM sodium chloride formulations is shown by the data in Table VI. Table VI shows the major metal oxides and the iron oxide impurity levels of typical borosilicate Type I glass. Up to 0.05% by weight (500 parts per million) (ppm)—iron oxide as Fe_2O_3 may exist in the borosilicate Type I glass (13). Thus, the increase in iron levels with time likely reflects a slow leaching of iron from the glass vial. Consistent with this explanation is that similar increases in silicon, aluminum, calcium and barium levels are also observed in older product lots, as shown in Table VI. Note that these non-transition metal ions are not known to participate in the type of reactions depicted in Figure 6.

Discussion

Iron, Citrate and Photons Catalytically Create Hydroxyl Radicals

All of the experimental observations are consistent with the scenario stated by Faust and Zepp (5) and depicted in Figure 12. Trace levels of iron in Drug A, 10 mM citrate (pH 6), 136 mM sodium chloride formulations increase with time. Solubilized iron complexes with citrate in the formulation. The oxidized iron (III)-citrate complex can be photoreduced to Fe^{2+} by exposure to either ICH visible or UV lamps (Figure 9). The Fe^{2+} reacts with dissolved oxygen in solution, as depicted in Figure 6, to form hydroperoxyl and ultimately hydroxyl radicals via the Fenton reaction. The hydroxyl radicals abstract hydrogen atoms from Drug A, leading to degradation products as shown in Figure 5. The Fe^{3+} formed can then be photoreduced repeatedly to Fe^{2+}, allowing for continued production

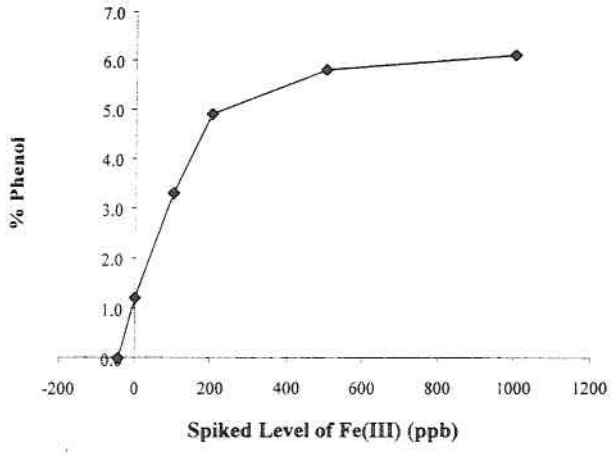

Figure 11

Percentage of drug loss observed for 0.57 mM Drug A in pH 6 10 mM citrate buffer after exposure to ICH visible lamp (1.2 million lux hours) in the presence of varying concentrations of iron. The level of iron present in the unspiked sample was determined by a standard addition method as 45 ppb (see Table V).

TABLE VI

Impurity Profiles of Borosilicate Glass and Corresponding ppb Levels of Elements Found in 3-month-old and 23-month-old 0.57 mM Drug A, 10 mM Citrate (pH 6), 136 mM Sodium Chloride Formulation Solutions Measured by ICP-MS

Metal Oxide	Impurity Profiles of Type I Borosilicate Glass, Water, and Two Different Product Batches				
	Clear Glass (ppm)	Amber Glass (ppm)	USP Water (ppb)	3-month-old (ppb)	23-month-old (ppb)
Silicon (as SiO_2)	685,000	664,000	100	300	3600
Aluminum (as Al_2O_3)	60,000	57,000	<1	28	470
Calcium (as CaO)	12,000	17,000	140	150	310
Barium (as BaO)	25,000	12,000	<2	10	120
Iron (as Fe_2O_3)	500	13,000	<2	5	45
Manganese (as MnO)	—	58,000	<2	<2	<2

of hydroxyl radicals from very low levels of iron. The catalytic role of the iron can be appreciated by examination of Table IV. In batch one, for example, the 1.2% levels of phenol formed were accompanied by about a 10% loss in the Drug A label claim. The lot contains near 50 ppb iron. Thus, the molar amount of Drug A lost is more than 60 times the molar amount of iron present. It is the photocatalytic nature of this chemistry that allows Fe levels of only 10s of ppb to oxidize significant quantities of Drug A. Furthermore, it is likely that at <200 ppb Fe levels in the Drug A formulation, iron is the limiting reagent and thus controls the level of photodegradation for a given light exposure. This is born out by the "linear" region of the slope in Figure 11. However, at >200 ppb iron levels, it is likely that oxygen becomes the limiting reagent and begins to control the apparent photodegradation reaction rate.

Implications for Control and Manufacture of Drug A Formulation I Solutions

The data described above clearly show that with time, Drug A Formulation I solutions will become more photosensitive due to increasing levels of iron in the product. The increase in photosensitivity over time

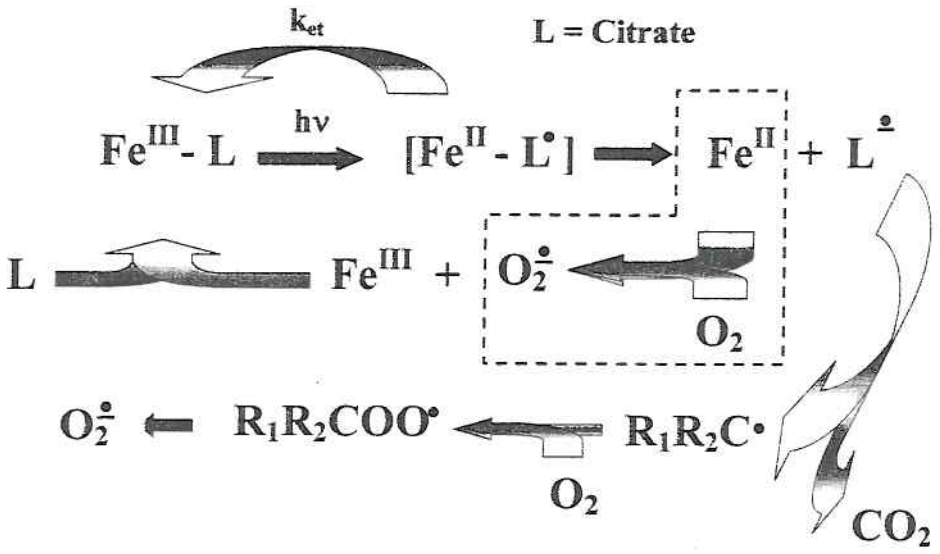

Figure 12

Photocatalytic scheme for Fe^{III} citrate mediated generation of Fe^{II}, which reacts with present oxygen to form two equivalents of superoxide radicals for every photon absorbed.

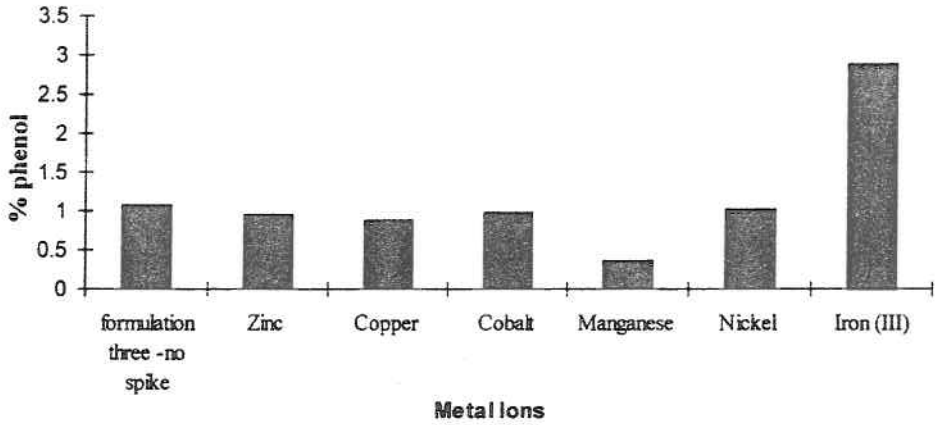

Figure 13

Percentage of phenol formed by spiking 100 ppb levels of various transition metals into 23-month-old product and exposing to ICH visible lamp (1.2 million lux hours). Note only 100 ppb iron spike showed any increased degradation compared to the unspiked control.

can be adequately addressed through the appropriate application of a secondary package to provide protection from light exposure during long-term storage.

Three primary questions remain. 1) How photosensitive are formulations at the point of manufacture? 2) How much light exposure might occur for a typical vial containing Drug A, Formulation I during manufacturing prior to placing each vial into a light-protective secondary package? 3) How can initial iron levels be controlled in successive formulations? These questions are framed within the context of a target <0.15% level for phenol in the product. Phenol levels measured after two years in dark stability chambers have been <0.1%, reflecting any contributions from the bulk drug substance (as an impurity), as well as thermal degradation that may have occurred over the two-year period. Therefore, about 0.1% levels of phenol can be tolerated due to photodegradation prior to individual packaging.

Iron is Likely the Primary Transition Metal of Concern at Initial Manufacture: The data described above clearly correlates the increase in photosensitivity with time to increased iron levels. However, at the time of initial manufacture, iron levels are lower. The best data available currently on initial iron levels is batch three, which has 5 to 10 ppb levels of iron 3 months after manufacture. A substantial portion of this iron is likely due to iron levels in the excipients, as described further below. All other transition metal ions are present at less than 1 ppb in the same lot. Iron is perhaps unique in its three-fold ability to 1) complex with citrate and be photoreduced, 2) react with oxygen in the reduced form to give superoxide radical, and 3) react in the reduced form with hydrogen peroxide to give hydroxyl radicals. Any transition metal ion must accomplish all three in order to give rise to the observed photodegradation. The uniqueness of iron is demonstrated in Figure 13, where salts of some of the more abundant transition metal ions (zinc, copper, cobalt, manganese, and nickel) were spiked into formulation I at 100 ppb levels and then exposed to ICH visible light stressing. None of the transition metals examined except iron showed increased formation of phenol compared to the unspiked sample of formulation I. Thus, it appears likely that iron levels will remain highly correlated with the photosensitivity of initially prepared Drug A Formulation I solutions.

Predictions of Phenol Levels from Iron Levels and Light Exposure: The photochemical generation of phenol levels in Drug A Formulation I solutions shortly after manufacture is therefore a function of both iron content and light exposure. The data in Figure 3 shows that phenol increases linearly with light exposure. The curve in Figure 11 also shows that phenol increases linearly over the 0–50 ppb iron levels at a fixed exposure of 1.2 million lux hours of visible light. Therefore, the formation of phenol can be predicted in the formulation as a function of both light and iron, as is illustrated in Table VIIa.

If one allows for a maximum of 0.15% of phenol from photodegradation that may occur prior to placing each vial into a light-protective secondary package, then the

TABLE VIIa
Predicted %Phenol Levels Predicted with Iron Content Under Unfiltered White Light Exposure

Iron (ppb)	Predicted Level of %Phenol at the Indicated Iron and Light Exposure									
	0.12[a]	0.24[a]	0.36[a]	0.48[a]	0.60[a]	0.72[a]	0.84[a]	0.96[a]	1.08[a]	1.2[a]
5	0.012	0.024	0.036	0.048	0.060	0.072	0.084	0.096	0.108	0.12
10	0.024	0.048	0.072	0.096	0.120	0.144	0.168	0.192	0.216	0.24
15	0.036	0.072	0.108	0.144	0.180	0.216	0.252	0.288	0.324	0.36
20	0.048	0.096	0.144	0.192	0.240	0.288	0.336	0.384	0.432	0.48
25	0.060	0.120	0.180	0.240	0.300	0.360	0.420	0.480	0.540	0.60
30	0.072	0.144	0.216	0.288	0.360	0.432	0.504	0.576	0.648	0.72
35	0.084	0.168	0.252	0.336	0.420	0.504	0.588	0.672	0.756	0.84
40	0.096	0.192	0.288	0.384	0.480	0.576	0.672	0.768	0.864	0.96
45	0.108	0.216	0.324	0.432	0.540	0.648	0.756	0.864	0.972	1.08
50	0.12	0.24	0.36	0.48	0.60	0.72	0.84	0.96	1.08	1.20

Note: The solid line represents the tolerance for light at a given iron level to allow 0.15% formation of phenol.
[a] Light exposure in units of million lux hours.

maximum light exposure for a given concentration of iron can be defined, as is shown in Table VIIa by the solid line. In general, control of iron to lower levels allows more flexibility with regard to the amount of light exposure that the product may receive without concern for appreciable photodegradation prior to packaging each vial in a light-protective secondary package.

Light mapping studies at two manufacturing sites have been performed to estimate the worst-case scenario for the amount of light exposure. Measurements at one site gave 0.12 million lux-hours (one-tenth of the visible ICH exposure) while the other site gave estimates of 0.21 million lux-hours. The value from site one represents the entire manufacturing and packaging exposure, while the other site value reflects only the manufacturing process and not the packaging time. If batch three is representative of manufacturing capability at 5 to 10 ppb iron, then Table VIIa shows that much higher light levels than those measured can actually be accommodated without problematic levels of phenol formation.

TABLE VIIb
Predicted %Phenol Levels Predicted with Iron Content Under Yellow Filtered White Light Exposure

Iron (ppb)	Predicted Level of %Phenol at the Indicated Iron and Light Exposure									
	0.12[a]	0.24[a]	0.36[a]	0.48[a]	0.60[a]	0.72[a]	0.84[a]	0.96[a]	1.08[a]	1.2[a]
5	0.002	0.004	0.006	0.008	0.010	0.012	0.014	0.016	0.018	0.020
10	0.004	0.008	0.012	0.016	0.020	0.024	0.028	0.032	0.036	0.040
15	0.006	0.012	0.018	0.024	0.030	0.036	0.042	0.048	0.054	0.060
20	0.008	0.016	0.024	0.032	0.040	0.048	0.056	0.064	0.072	0.080
25	0.010	0.020	0.030	0.040	0.050	0.060	0.070	0.080	0.090	0.100
30	0.012	0.024	0.036	0.048	0.600	0.072	0.084	0.096	0.108	0.120
35	0.014	0.028	0.042	0.056	0.070	0.084	0.098	0.112	0.126	0.140
40	0.016	0.032	0.048	0.064	0.080	0.096	0.112	0.128	0.144	0.160
45	0.018	0.036	0.054	0.072	0.090	0.108	0.126	0.144	0.162	0.180
50	0.020	0.040	0.060	0.080	0.100	0.120	0.140	0.160	0.180	0.200

Note: The solid line represents the tolerance for light at a given iron level to allow 0.15% formation of phenol.
[a] Light exposure in units of million lux hours.

TABLE VIII
Possible Contributions to Iron Levels in the Formulation from Drug and Excipients at Product Manufacture

Component	Contribution to Concentrate at Specified Iron Level for Component				
	1 ppm	2 ppm	3 ppm	5 ppm	"Best"
Drug A	0.3 ppb	0.6 ppb	0.9 ppb*	1.5 ppb	0.9 ppb
Citric Acid	0.1 ppb	0.3 ppb	0.4 ppb*	0.6 ppb	0.4 ppb
Sodium Citrate	2.7 ppb	5.4 ppb	8.1 ppb	13.5 ppb*	13.5 ppb
Sodium Chloride	8 ppb*	16 ppb	24 ppb	40 ppb	8 ppb
Water	—	—	—	—	—
Total	11 ppb	22 ppb	33 ppb	56 ppb	23 ppb

* Indicates the level specified in best quality commercially available material.

Alternatively, the benefits of incorporation of yellow light filters (or replacing white light with yellow light sources) can be considered for manufacturing and packaging areas. In this analysis, the ICH photo-chamber was modified to filter visible light through a representative yellow film common in manufacturing/packaging facilities. The light transmission properties of the specific film used in this study (UV cut off at 540 nm) is shown in Figure 9 (—·—·—). The overall benefit resultant of reducing light exposure specific to the ligand-to-metal charge transfer transition for iron (III) citrate is a six-fold reduction in the amount of photodegradation for a given light and iron combination (Table VIIb). The yellow light conditions significantly increase the tolerance for light exposure and iron content for this formulation.

Control of Iron Levels in Liquid Formulations: The most logical way to ensure adequate light stability during the manufacturing and packaging process is to control the levels of iron present in the excipients in the formulation. Currently, iron content is only controlled in the sodium chloride that is used in the formulation at ≤2 ppm. Iron is not controlled in citric acid, sodium citrate, the bulk drug substance, nor the water. The addition of iron specification controls for the solid components in the formulation are analyzed in Table VIII. Across the board specifications of 2 ppm iron for each excipient, for example, would give rise to a maximum of 22 ppb iron in the product, assuming each solid component contained iron at the 2 ppm specification limit and that negligible amounts of iron (< several ppb) are present in the water. Sodium chloride will dominate the iron contribution if all solid components have the same iron specification, as shown in Table VIII. A quick survey of typical specifications for maximum iron levels allowed in commercially available materials are noted in Table VIII by asterisks (*) and are 3 ppm, 5 ppm, and 1 ppm for citric acid, sodium citrate, and sodium chloride, respectively. The maximum possible iron in product due to use of these excipients would be 22 ppb iron, as shown in the right hand column. The fact that batch three contains only 5 to 10 ppb iron levels clearly indicates the *actual* iron levels in our excipients, including water, are significantly below the label-specified limits.

The water used in the formulation could potentially contribute significantly, and will require iron levels below the maximum-allowed ppb iron limit desired in the product. Table VII and Table VIII provide the basis for determining iron control limits for excipients and water, in addition to allowed light exposure limits. Greater tolerance in the specifications for iron in the excipients requires tighter control of the light exposure allowed, and vice versa. Together, appropriate iron and light exposure controls can assure continued successful manufacturing batches with negligible phenol levels at the time of final packaging.

Generality of the Observed Photodegradation

The Photocatalytic Chemistry is General to Polycarboxylate Buffers: The photodegradation of Drug A Formulation I solutions at a fixed iron content was examined for a series of 10 mM polycarboxylate buffers (oxalate, succinate, maleate, tartrate, and formate). The general photocatalysis was observed for all systems examined and varied from 0.40 % to 17.6 % loss of Drug A for a 50-ppb level of iron present (Table

TABLE IX
Visible Photo-Degradation of Drug A as a Function of Carboxylate Buffer System

Buffer[a]	% Drug A Loss Estimated as a Function of ppb Iron			
	PKa's[b]	1 ppb Iron	10 ppb Iron	50 ppb Iron
Oxalate	1.3, 4.3	0.351	3.51	17.6
Succinate	4.2, 5.6	0.014	0.14	0.70
Maleate	1.9, 6.3	0.011	0.11	0.55
Tartrate	3.0, 4.4	0.071	0.71	3.55
Citrate	3.1, 4.8, 6.4	0.187	1.87	9.35
Formate	3.8	0.008	0.08	0.40

[a] Buffers were adjusted to pH 6, and solutions were 10 mM for each specified buffer, Drug A was maintained at 0.57 mM and 1.2 million lux of visible light exposure was provided to each solution.
[b] Pka values were taken from Lange's Handbook of Chemistry, 14th Edition, pp. 8.19–8.71.

IX). The following order of photosensitivity was observed:

oxalate > citrate > tartrate > succinate ~ maleate ~ formate

The observed photosensitivity order above does not appear to correlate with the reported quantum yields of some of these carboxylate complexes (Table X), signaling the significance of the pH dependence of the recombination reactions.

In all cases examined, the level of photodegradation in the presence of 50 ppb iron (representative of potential iron amount after 2 years storage in borosilicate glass) could have significant impact on the photostability of a product and may introduce the need to take steps to protect the product from light. At manufacture, signified by the 10 ppb levels, succinate, maleate and formate formulations would likely have acceptable photostability to minimize the need for light exposure control during manufacturing and packaging operations.

The Photodegradation Chemistry is General to Other Drug Compounds: The generality of the ability of the iron-citrate-oxygen system to create hydroxyl radicals capable of oxidizing drug substances in solution was examined for a series of four drugs: 1) Drug A (a phenyl ether: no light absorption above 300 nm), 2) Drug B (a phenyl piperidone: significant light absorption above 300 nm), 3) Drug C (an alkyl pip-

TABLE X
Quantum Yields of the Fe^{II} Generation for Fe^{III} Complexes of Carboxylate Buffers at pH 2.7 and pH 4.0. (Taken from H. B. Abrahamson, A. B. Rezvani and G. Brushmiller, *Inorg. Chim. Acta*, 226 (1–2), 117–127, 1994, unless otherwise noted.)

Buffer	PKa's[c]	Quantum Yield[a]		Complexation Constant[b]		
		pH = 2.7	pH = 4.0	# Ligands	Fe^{III}	Fe^{II}
Oxalate	1.3, 4.3	0.65	0.30	2, 3	16.2, 20.2	4.5, 5.2
Succinate	4.2, 5.6				7.5	
Maleate	1.9, 6.3	0.21	0.29	2, 3	15.5	4.4
Tartrate	3.0, 4.4	0.35	0.50		7.5	
Citrate	3.1, 4.8, 6.4	0.28	0.45	1	12.5	3.1
Isocitrate	3.1, 4.8	0.14	0.37			

[a] Quantum Yield with ligand to iron ratio of five to one. Measurements were made with 366 nm irradiation in the absence of oxygen, using phenanthroline as a complexing agent for iron.
[b] Lange's Handbook of Chemistry, 14th edition, pp. 8.89–8.103.
[c] Pka values were taken from Lange's Handbook of Chemistry, 14th Edition, pp. 8.19–8.71.

TABLE XI
Visible Photo-Degradation of Drugs A–D in 10 mM Citrate Buffer

Formulation[a]	% Drug Loss Estimated as a Function of ppb Iron			
	Buffer	1 ppb Iron	10 ppb Iron	50 ppb Iron
Drug A	10 mM Citrate	0.429	4.29	21.4
(phenyl ether)	pH 3.0			
Drug B	10 mM Citrate	0.394	3.94	19.7
(phenyl piperidone)	pH 3.0			
Drug C	10 mM Citrate	0.288	2.88	14.4
(alkyl piperidone)	pH 3.0			
Drug D	10 mM Citrate	0.137	1.37	6.85
(phenyl thiazole)	pH 2.5			

[a] Buffers were adjusted to pH 3, with the exception of Drug D where the pH was adjusted to pH 2.5 to maintain adequate solubility. Each drug concentration was maintained at 0.57 mM and 1.2 million lux of visible light exposure was provided to each solution.

eridone: no light absorption above 300 nm), and 4) Drug D (a phenyl thiazole: significant light absorption above 300 nm). All formulations were made at 0.57 mM drug concentration in 10 mM citrate, pH 3 for Drug A, B and C, and pH 2.5 (slightly more acidic due to solubility limitations) for Drug D, and placed in clear USP Type I glass vials. All solutions were then exposed to 1.2 million lux hours of visible light in the ICH chamber with levels of iron spiked into each preparation. In each case, the level of iron present was determined to account for contributions from excipients and the drug itself. The amount of drug loss observed with 50 ppb levels of iron present ranged from 6.85% to 21.4% and is considered significant for all formulations (Table XI). Even at 10 ppb Fe levels, the amount of degradation observed is also significant enough to effect light exposure concerns in manufacturing and packaging areas, and would likely require a light-protective package. The generality of the photodegradation is expected, and strongly supports hydroxyl radicals as the key reactive species since many types of C–H bonds are susceptible to hydrogen atom abstraction by hydroxyl radicals.

The Significance of the Photodegradation is Highly Dependent on the Formulation Drug Concentration

The dependence of the percentage of drug lost on the initial drug concentration was examined in the 10 mM citrate (pH 6), 50-ppb iron system spanning from 1 to 500 mM Drug B concentrations. Again, all formulations were placed in clear USP type I glass vials and the iron content of each formulation was measured, followed by exposure to 1.2 million lux hours of visible light. Figure 14 illustrates that the extent of photodegradation becomes increasingly less significant at increasing drug concentrations, becoming largely insignificant at 100 mM concentrations and above. The trend in Figure 14 is consistent with the observed limitation iron plays at the <200 ppb levels (Figure 11), where a fixed quantity of drug can be consumed at a given iron level and light exposure.

Conclusions

The iron-mediated photodegradation of solutions containing polycarboxylate buffers has been shown to be

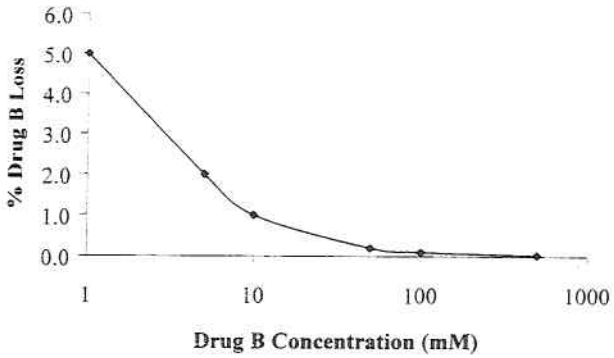

Figure 14

Percentage of drug loss observed for varying concentrations of Drug B in pH 6 10 mM citrate buffer after exposing to ICH visible lamp (1.2 million lux hours) in the presence of 50 ppb iron.

generally relevant to a wide range of drug substances. The presence of iron has also shown to be ubiquitous, as iron is present in drug substances, raw materials, and packaging materials. In the present case, the photodegradation observed is significant at ppb levels of iron and thus protection from light is required during manufacturing, packaging operations, and shelf storage.

Acknowledgments

We gratefully acknowledge Qingxi Wang and Shyam Karki for conversations concerning Fenton chemistry, Shyam Karki for initiating the literature search on the photochemistry of citrate complexes, and John Ballard for obtaining mass spectral data on the concentrated, desalted sample provided.

References

1. For example, see B. Halliwell, J. M. C. Gutteridge, "Free Radicals in Biology and Medicine," 2nd ed; Oxford University Press:, Oxford, UK,1989; pp 36–104.

2. J. G. Neilands, Evolution of Biological Iron Binding Centers. *Struct. Bonding* **11,** 145–170 (1972).

3. For example, see H. B. Abrahamson, A. B. Rezvani, G. Brushmiller, Photochemical and spectroscopic studies of complexes of iron (III) with citric acid and other carboxylic acids. *Inorg. Chim. Acta.* **226**(1–2), 117–127 (1994), and references therein.

4. B. Halliwell, J. M. C. Gutteridge, "Free Radicals in Biology and Medicine," 3rd ed. Oxford University Press: Oxford, UK, 1991; pp 401–406.

5. B. Faust, R. G. Zepp, Photochemistry of Aqueous Iron (III)-Polycarboxylate Complexes: Roles in the Chemistry of Atmospheric and Surface Waters. *Environ. Sci. Tech.* **27**(12), 2517–2522 (1993).

6. For example, see *Advances in Catalysis,* 1st ed; D. D. Eley, H. Pines, P. Weisz, Eds.; Academic Press: New York, NY, 1976; Vol. 25, pp 25–56.

7. J. J. Llorens-Molina, Photochemical reduction of Fe3+ by citrate ion. *J. Chem. Educ.* **65**(12), 1090 (1988).

8. International Conference on Harmonization. Guidelines for the Photostability Testing of New Drug Substances and Products. *Federal Register* **62,** 27115–27122 (1997).

9. P. Helboe, The Elaboration and Application of the ICH Guideline on Photostability:A European View. In *Drugs: Photochemistry and Photostability;* Royal Society of Chemistry: London, UK, 1998; pp 243–247.

10. S. R. Thatcher, R. K. Mansfield, R. B. Miller, C. W. Davis, S. W. Baertschi, Pharmaceutical Photostability: A Technical Guide and Practical Interpretation of the ICH Guideline and Its Application to Pharmaceutical Stability—Part 1. *Pharmaceutical Technology* **25**(3), 98–110 (2001).

11. S. R. Thatcher, R. K. Mansfield, R. B. Miller, C. W. Davis, S. W. Baertschi, Pharmaceutical Photostability: A Technical Guide and Practical Interpretation of the ICH Guideline and Its Application to Pharmaceutical Stability—Part 2. *Pharmaceutical Technology* **25**(4), 50–62 (2001).

12. For example, see (a) D. E. Moore, Photophysical and Photochemical Aspects of Drug Stability. In *Photostability of Drugs and Drug Formulations:* Taylor and Francis: London, UK, 1996; pp 9–38. (b) K. Thoma, Photodecomposition and Stabilization of Compounds in Dosage Forms. In *Photostability of Drugs and Drug Formulations;* Taylor and Francis: London, UK, 1996; pp 111–140.

13. Monograph on Citric Acid. In *Encyclopedia of Chemical Technology;* 4th edition; John Wiley & Sons: New York, NY, 1993; Vol. 4, pp 354–380.